

† Supporting Information for

Electrochemically Shape-Controlled Synthesis of Trapezohedral Platinum Nanocrystals with High Electrocatalytic Activity

Yanyan Li, Yanxia Jiang*, Minghui Chen, Honggang Liao, Rui Huang, Zhiyou Zhou, Na Tian, Shengpei Chen and Shigang Sun*

State Key Laboratory of Physical Chemistry of Solid Surfaces, Department of Chemistry, College of Chemistry and Chemical Engineering, Xiamen University, Xiamen 361005, (P. R. China)
Email: sgsun@xmu.edu.cn

1. Reagents and materials

Hexachloroplatinic acid hexahydrate ($\text{H}_2\text{PtCl}_6 \cdot 6\text{H}_2\text{O}$, A.R. reagent), H_2SO_4 (G.R. reagent), formic acid (A.R. reagent), methanol (A.R. reagent) were purchased from Sinopharm Chemical Reagent Co. Ltd. (Shanghai, China). Millipore water ($18.2 \text{ M}\Omega \cdot \text{cm}$) provided by a Milli-Q Labo apparatus (Nihon Millipore Ltd.) was used in all experiments. All reagents were used as received without further purification. Nafion solution (5%) was purchased from Dupont Corporation. The Pt/XC-72 catalyst (commercial Pt/C) with 20 wt % total metal loading was obtained from the Johnson Matthey Corporation, which was used for comparison.

2. Catalyst characterization

The surface structure of the trapezohedral Pt nanoparticles crystals (TPH Pt NCs) was characterized by the scanning electron microscopy (SEM, Hitachi S-4800 SEM) and transmission electron microscopy (TEM, Tecnai F30, JEM-2100). HRTEM studies were performed on a Tecnai F30 high-resolution transmission electron microscope operating at 300 kV.

3. Electrochemical Measurements

Electrochemical experiments were carried out in a standard three-electrode cell at room temperature (about 25°C). The counter electrode was a foil of platinized platinum and reference electrode was a saturated calomel electrode (SCE). All electrode potentials were quoted versus the saturated calomel electrode (SCE). Glassy carbon rod (GC, 6.0 mm in diameter and 10.0 mm long) was purchased for Takai Carbon Co. Ltd. (Tokyo, Japan). The GC rode was sealed with Teflon and only one end was exposed during the electrochemical experiment. The GC electrode was polished mechanically by using successively sand paper (6 #) and alumina power of size 5, 1, and $0.3 \mu\text{m}$, and then washed with Millipore water in an ultrasonic bath. The three-electrode electrochemical cell was connected to a PAR 263A potentiostat (EG&G) to control electrode potential. The solution was deaerated by bubbling high-purity N_2 for 20 min before measurements, and this atmosphere was maintained by a flow of N_2 gas over the solution during the experiment. The TPH Pt NCs was prepared by direct electrodeposition in $1 \text{ mg mL}^{-1} \text{H}_2\text{PtCl}_6 \cdot 6\text{H}_2\text{O} + 0.5 \text{ M H}_2\text{SO}_4$ solution through a potential program shown in Fig. S1. The commercial Pt/C catalyst of 5 mg used for comparison was ultrasonically dispersed in Millipore water of 5 mL (1 mg mL^{-1}) to form the catalyst ink, which was dropped on the GC electrode and left to dry. Then Nafion was covered on the Pt/C film.

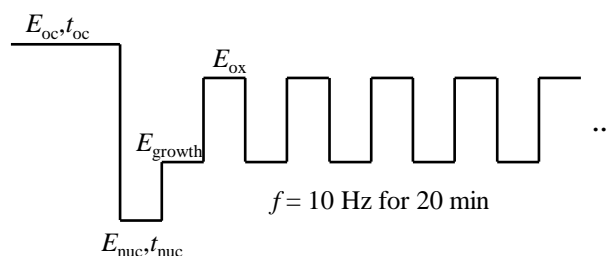


Fig. S1 Potential program of direct electrochemical deposition for TPH Pt NCs, in which E_{oc} is the cleaning potential, E_{nuc} is the potential of producing Pt nuclear, E_{growth} is the potential of Pt growth, E_{ox} is the potential of oxygen adsorption.

The direct electrodeposition is different from the two-step procedure developed previously for the preparation of THH Pt NCs,¹ and it is straightforward and simple in electrochemically shape-controlled synthesis of metal nanoparticles of high surface energy. In this approach, the nuclei were formed at first at the nucleation potential (-0.3 V , Fig. S1), and then a square wave potential was applied to the growth of Pt nanoparticles. The lower and upper limit potentials in the square wave corresponding respectively to the potential of the growth (E_{growth}) and the oxidation potential (E_{ox}) are both critical in controlling the surface structure (thus the shape) of the Pt NCs. The E_{growth} proceeds the growth of Pt NCs, while the E_{ox} induces the reconstruction of the Pt atoms. The adsorption and reduction of Pt ions at E_{growth} and oxygen at E_{ox} on Pt NCs reduces surface energy of high-index facets and consequently stabilizes the Pt NCs of high surface energy. The E_{growth} , E_{ox} and the concentration of processor control the kinetics of Pt growth, resulting in tuning the shape of Pt NCs.

4. The method and analysis of direct electrochemical deposition of TPH Pt NCs

Glassy carbon electrode (GC) possesses the low surface energy, which allows metal nanoparticles growth preferentially to individual particles or clusters through the Volmer-Weber mode,² so the GC surface favors the shape-controlled synthesis of metal nanocrystals.¹

5. The equilibrium potentials of the couple $\text{PtCl}_6^{2-}/\text{Pt}$ on theoretical and experimental values

The equilibrium potentials are 0.726 V and 0.758 V in the following two electrode reactions,



Electrode potential of half-cell reaction:



can be calculated from the conservation of energy, we have:

$$E_3 = (G_1 + G_2)/(n_1 + n_2)F = (n_1FE_1 + n_2FE_2)/(n_1 + n_2)F = (2 \times 0.726 + 2 \times 0.758)/4 = 0.742 \text{ (V)},$$

So standard electrode potential of the couple $\text{PtCl}_6^{2-}/\text{Pt}$ is calculated to be 0.742 V vs. SHE, and 0.501 V vs. SCE. The open circuit potential of $\text{PtCl}_6^{2-}/\text{Pt}$ in $1 \text{ mg mL}^{-1} \text{ H}_2\text{PtCl}_6 \cdot 6\text{H}_2\text{O} + 0.5 \text{ M H}_2\text{SO}_4$ solution is determined to be 0.659 V. They are consistent with the deposition curve (Fig. S2).

GC possesses the low surface energy, resulting in the deposition of Pt on the GC has a higher overpotential (Fig. S2). Therefore, the reduction of PtCl_6^{2-} at 0.25 V only keep Pt NCs growing on the Pt nuclei produced at -0.3 V. No any new nuclei could be generated at the high reduction potential of 0.25 V. In addition, the reduction of PtCl_6^{2-} stops at 1.0 V, while the consumption of PtCl_6^{2-} on electrode surface can be provided by the PtCl_6^{2-} ion diffusion. In the meantime the oxygen adsorption on Pt NCs induce the formation of high-index facets, so that the uniform TPH Pt NCs with both shape and size have been controlled by the program shown in Fig. S1.

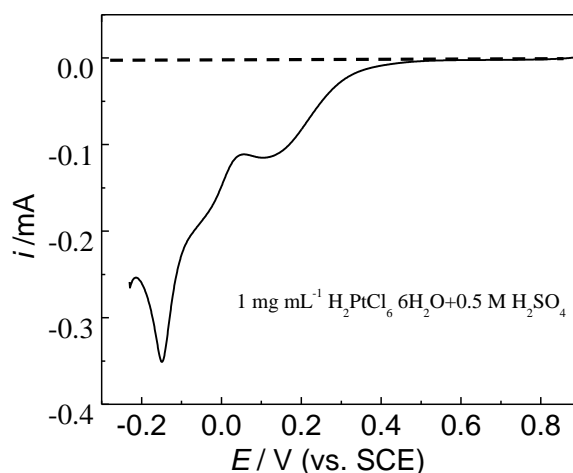


Fig. S2 Linear scan curve of Pt deposition on GC substrate electrode in solution of $1 \text{ mg mL}^{-1} \text{ H}_2\text{PtCl}_6 \cdot 6\text{H}_2\text{O} + 0.5 \text{ M H}_2\text{SO}_4$, scan rate: 50 mV s^{-1} .

6. The characterizations of TPH Pt NCs

SEM images of the Pt TPH NCs showed in Fig. S3. In this square-wave method, the nuclei were formed at the nucleation potential of -0.3 V, and then potential of 0.25 V was applied to the growth of Pt nanoparticles. The potential of the growth (E_{growth}) is so positive that the Pt nanoparticles mainly to growth, not to form the new nuclei. Therefore almost of the Pt NCs is TPH shape (Fig. S3b), the particle size is also uniform, and finally we can get a high yield TPH Pt NCs (Fig. S3a). From Fig. S3c we can see that the TPH Pt NCs have good stability after electrocatalysis examinations.

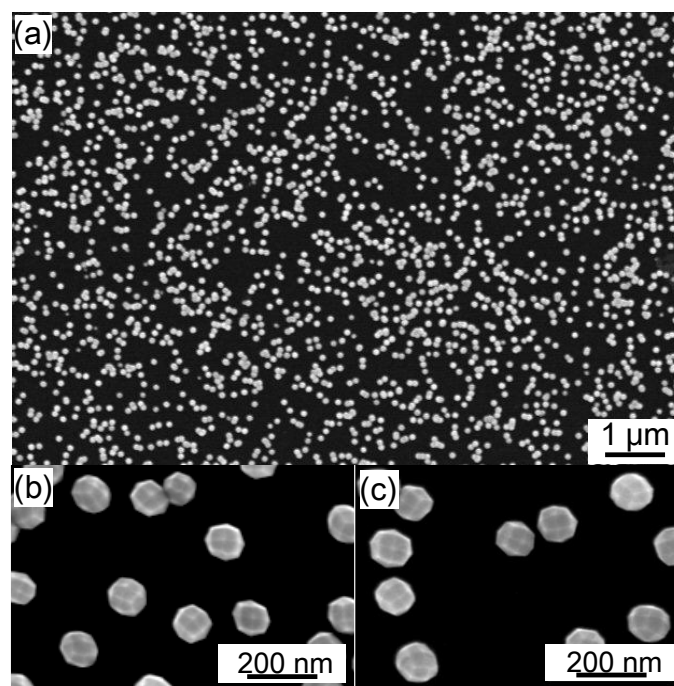


Fig. S3 (a) Scanning electron microscopy (SEM) images of the as-prepared TPH Pt NCs with the Large-area, (b) enlarged of (a), and (c) SEM images of the TPH Pt NCs after electrocatalysis examinations. E_{nuc} : -0.30 V for 20 ms, E_{growth} : 0.25 V, E_{ox} is 1.0 V, f is 10 Hz for 20 min, in $1\text{ mg mL}^{-1} \text{H}_2\text{PtCl}_6 \cdot 6\text{H}_2\text{O} + 0.5 \text{ M H}_2\text{SO}_4$ solution.

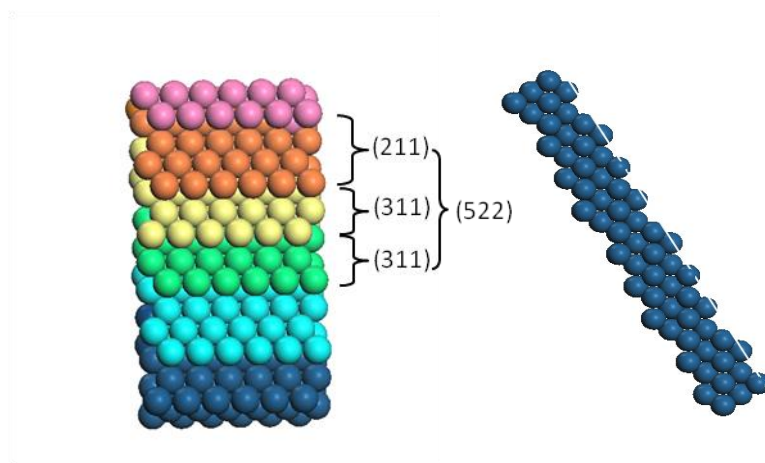


Fig. S4 Atomic arrangement of (522) facet, with models of viewing the surfaces from top (a) and side (b). An ideal Pt (n+1, n-1, n-1) surface consists of an ordered staircase of steps separated by (100) step edges. The corresponding terrace-step notation for a Pt (n+1, n-1, n-1) surface is Pt (S)-[n(111) × (100)]. n represents the width in the number of (111) terrace atoms. An (522) facet of fcc Pt is periodically composed of (211) and (311) subfacets.

$$\text{Pt}(211) = \text{Pt}(\text{S}) - [3(111) \times (100)],$$

$$\text{Pt}(311) = \text{Pt}(\text{S}) - [2(111) \times (100)],$$

$$\text{Pt}(522) = \text{Pt}(\text{S}) - [2(311) \times (211)].$$

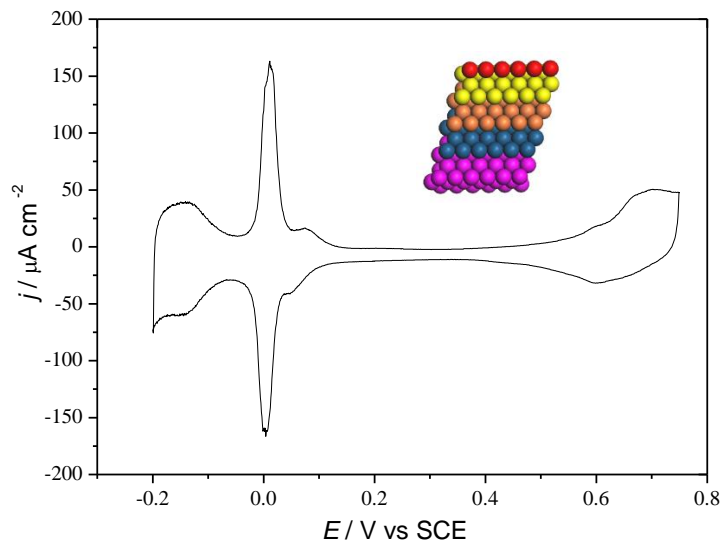


Fig. S5 Cyclic voltammogram of Pt(311) electrode in 0.5 M H₂SO₄ solution, sweep rate 50 mV s⁻¹.

Table S1 List of Angles and determined from Fig. 2b

Number	1	2	3	4	Average
Angle	135.15	136.70	137.95	137.87	136.9
Angle	134.66	130.50	132.39	134.36	133.0

Table S2 Theoretical parameters of trapezohedral nanocrystals bounded by different high-index (hkk) Facets. ($\alpha = 2 \arctan(h/k)$)

Miller Indices (hkk)	(211)	(733)	(522)	(311)
Angle	126.9	133.6	136.4	143.2
Angle	143.1	136.4	133.6	126.8

References:

- (a) N. Tian, Z. Y. Zhou, S. G. Sun, Y. Ding and Z. L. Wang, *Science*, 2007, **316**, 732; (b) N. Tian, Z. Y. Zhou, N. F. Yu, L. Y. Wang and S. G. Sun, *Journal of the American Chemical Society*, 2010, **132**, 7580-7581; (c) N. Tian, Z. Y. Zhou and S. G. Sun, *Chem. Commun.*, 2009, 1502-1504.
- E. Walter, B. Murray, F. Favier, G. Kaltenpoth, M. Grunze and R. Penner, *The Journal of Physical Chemistry B*, 2002, **106**, 11407-11411.